European Society for Paediatric Research
Society for Pediatric Research
www.nature.com/pr

BASIC SCIENCE ARTICLE

Check for updates

Fetal pulmonary hypertension: dysregulated microRNA-34c-Notch1 axis contributes to impaired angiogenesis in an ovine model

Devashis Mukherjee[1], Ujala Rana[2], Alison J. Kriegel[3], Pengyuan Liu[3], Teresa Michalkiewicz[2] and Girija Ganesh Konduri[2]✉

BACKGROUND: Persistent pulmonary hypertension of the newborn (PPHN) occurs when pulmonary vascular resistance (PVR) fails to decrease at birth. Decreased angiogenesis in the lung contributes to the persistence of high PVR at birth. MicroRNAs (miRNAs) regulate gene expression through transcript binding and degradation. They were implicated in dysregulated angiogenesis in cancer and cardiovascular disease.
METHODS: We investigated whether altered miRNA levels contribute to impaired angiogenesis in PPHN. We used a fetal lamb model of PPHN induced by prenatal ductus arteriosus constriction and sham ligation as controls. We performed RNA sequencing of pulmonary artery endothelial cells (PAECs) isolated from control and PPHN lambs.
RESULTS: We observed a differentially expressed miRNA profile in PPHN for organ development, cell–cell signaling, and cardiovascular function. MiR-34c was upregulated in PPHN PAECs compared to controls. Exogenous miR34c mimics decreased angiogenesis by control PAEC and anti-miR34c improved angiogenesis of PPHN PAEC in vitro. Notch1, a predicted target for miR-34c by bioinformatics, was decreased in PPHN PAECs, along with Notch1 downstream targets, Hey1 and Hes1. Exogenous miR-34c decreased Notch1 expression in control PAECs and anti-miR-34c restored Notch1 and Hes1 expression in PPHN PAECs.
CONCLUSION: We conclude that increased miR-34c in PPHN contributes to impaired angiogenesis by decreasing Notch1 expression in PAECs.

Pediatric Research (2023) 93:551–558; https://doi.org/10.1038/s41390-022-02151-3

IMPACT:

- Adds a novel mechanism for the regulation of angiogenesis in persistent pulmonary hypertension of the newborn.
- Identifies non-coding RNAs that are involved in the altered angiogenesis in PPHN and thus the potential for future studies to identify links between known pathways regulating angiogenesis.
- Provides preliminary data to conduct studies targeting miR34c expression in vivo in animal models of pulmonary hypertension to identify the mechanistic role of miR34c in angiogenesis in the lung vasculature.

INTRODUCTION

Persistent pulmonary hypertension of the newborn (PPHN) is characterized by dysregulation of angiogenesis in the lung, resulting in failure of postnatal decrease in pulmonary vascular resistance (PVR).[1–4] In utero, blood from the right ventricle crosses from the pulmonary artery (PA) to the aorta (Ao) across the patent ductus arteriosus (PDA) due to elevated PVR. Failure of postnatal decrease in PVR leads to persistence of the fetal circulation leading to hypoxemia, cyanosis, and the need for supplemental oxygen, mechanical ventilation, or possibly extracorporeal life support. Currently, inhaled nitric oxide is the only Food and Drug Administration–approved therapy for neonates with hypoxemic respiratory failure secondary to PPHN. Animal models of PPHN have shown impaired angiogenesis to be a key factor contributing to elevated PVR.[1–4] Angiogenesis is the process by which endothelial cells (ECs) lining existing blood vessels sprout and form new vessels.[5] Dysregulation in either EC signaling or downstream pathways or both leads to decreased angiogenesis, resulting in elevated PVR in PPHN. We previously reported that in fetal lambs, in utero ligation of the PDA for 7–8 days results in a phenotype resembling human PPHN with significantly increased PVR, pruning of the pulmonary vasculature, and decreased angiogenesis.[3,4] Pulmonary artery ECs (PAECs) isolated from these fetal lambs show decreased angiogenesis in vitro.[2–4] We and others reported downregulation of several key mediators, including endothelial nitric oxide synthase and 5′-adenosine monophosphate-activated protein kinase and increased reactive oxygen species in this model.[2,6,7] The role of non-coding

[1]Department of Pediatrics, Rainbow Babies and Children's Hospital, Case Western Reserve University School of Medicine, Cleveland, OH, USA. [2]Department of Pediatrics and Children's Research Institute, Medical College of Wisconsin and Children's Wisconsin, Milwaukee, WI, USA. [3]Department of Physiology, Medical College of Wisconsin, Milwaukee, WI, USA. ✉email: gkonduri@mcw.edu

Received: 24 December 2021 Revised: 17 May 2022 Accepted: 26 May 2022
Published online: 18 June 2022

ribonucleic acids (RNAs) and post-transcriptional modification of gene expression in the pathogenesis of altered angiogenesis in PPHN is unknown.

MicroRNAs (miRNAs) are 22-nucleotide long, non-coding RNAs that are mostly conserved across species.[8] MiRNAs are synthesized as double-stranded sequences in the nucleus. They have a 2–8 base-long "seed" region that is complementary to and binds the 3′ untranslated region (3′UTR) of messenger RNAs (mRNAs) leading to transcript degradation or repression of protein translation.[9] Since their discovery, they have been implicated in a multitude of diseases where angiogenesis is impaired including cancer, atherosclerotic disease, vasculopathies, and pulmonary hypertension.[8,10,11] MiRNAs are synthesized in the nucleus by RNA polymerase II as a double-stranded long transcript known as primary miRNA transcript that subsequently gets cleaved into a ~70-nucleotide precursor miRNA (pre-miRNA) by an RNAse II-type protein, Drosha.[9] Pre-miRNA is exported out of the nucleus by Exportin-5 into the cytoplasm where it undergoes further cleavage by Dicer to form the double-stranded RNA complex containing the mature miRNA strand and its complementary sequence. This is bound by transactivating RNA-binding protein and Argonaute protein to form the RNA-induced silencing complex (RISC). The mature miRNA strand guides the RISC to the 3′UTR of a specific mRNA based on the degree of complementarity between the seed region of the miRNA and the 3′UTR. RISC subsequently inhibits translation, highlighting the importance of miRNAs in post-transcriptional modification.

MiRNAs have been implicated in several animal models of pulmonary hypertension.[12,13] Those belonging to the miR-17–92 cluster, specifically miR-17 and miR-92a contribute to dysregulated EC function and angiogenesis.[14,15] Rat hypoxia models of PH have shown that increased miR-126a contributes to the hypoxia-induced endothelial-to-mesenchymal transition in neonatal PH.[16] MiR-126a has also been shown to be involved in Klf-2a-mediated activation of vascular endothelial growth factor (VEGF) signaling.[17] MiR-21 was found to be a likely contributor to pulmonary vascular remodeling due to hypoxia and targets bone morphogenetic protein receptor-2.[18] Other miRNAs like miR-145 and miR-210 are also upregulated in experimental models and contribute to pulmonary artery smooth muscle cell (PASMC) migration and proliferation and PAEC proliferation and resistance to apoptosis. Microarray analysis from postmortem lung tissue of infants who died from PPHN identified miR-379, miR-7977, and miR-455 to be significantly downregulated.[19] Changes in miRNA profile in neonatal PPHN and whether these serve as biomarkers of dysregulated angiogenesis or are involved in post-transcriptional modification of key signaling pathways in PPHN remains unknown. Our objective of this study was to identify the differential miRNA expression between control and PPHN lamb PAECs and to study the in vitro effects of altering the expression of these miRNAs on angiogenesis.

METHODS

Generation of PPHN lamb model and extraction of PAECs

Animal studies were approved by the Medical College of Wisconsin Institutional Animal Care and Use Committee and conformed to current National Institutes of Health guidelines for care and use of laboratory animals. Fetal ductus arteriosus constriction was performed at 128 ± 2 days of gestation (full term being ~142 days) to generate PPHN phenotype as described previously.[20,21] A sham surgery without ductal ligation was performed to generate control phenotype. After 8 days of ductal constriction, pregnant ewes were euthanized, fetuses were delivered, and lungs were removed en bloc from them. PAECs were isolated using 0.1% collagenase type A from the main pulmonary arteries and immunopurified using CD31 antibody-coated magnetic beads. Their identity was verified by staining for factor VIII antigen and acetylated low-density lipoprotein uptake.[4,22,23]

Next-generation sequencing

Total RNA was extracted from passage two PAECs harvested from six each control and PPHN lambs (three male and three female in each group) using TRIzol (Thermo Fisher Scientific Inc., Waltham, MA) method as described previously.[24] Small RNA libraries were prepared using Illumina TruSeq Small RNA Sample Preparation kit. Amplified complementary DNA (cDNA) constructs after separation on 6% polyacrylamide gel electrophoresis were purified and used for small RNA sequencing using Illumina HiSeq 4000. Data were analyzed as described previously.[25,26] The cleaned sequences were mapped against miRBase v19 to identify known miRNAs (sheep miRNAs and homologs of miRNAs known in species other than the sheep) using miRanalyzer.[27] Differential expression of miRNAs was detected using DESeq2.[28] The Benjamini–Hochberg method was used to control false discovery rate (FDR) in all statistical tests.[29] FDR of 0.05 was deemed as significant.

Identification of microRNAs for study

RNA-sequencing data were analyzed to find miRNAs that had a significant fold change in the PPHN PAECs as compared to the control PAECs. Ingenuity pathway analysis (IPA, Qiagen, Germantown, MD) was used to identify molecular and cellular functions as well as the top analysis-ready miRNAs. IPA was also used to identify the top analysis-ready up and downregulated miRNAs. These were input into open-access software, TargetScan to identify predicted mRNA targets for each miRNA based on the complementarity between the miRNA seed region and the mRNA 3′UTR.[28] MiRNAs that had targets in pathways known to be involved in angiogenesis, cell signaling, and cell proliferation based on data from IPA and TargetScan were selected for further study.

Cell culture and microRNA transfection

Fetal lamb PAECs between passages 2–5 were cultured in Dulbecco's Modified Eagle's Media (DMEM) supplemented with 20% fetal bovine serum, in a humidified incubator at 37 °C, 5% CO_2, and 95% room air. Transfection was carried out at 60–70% confluency using miRNA mimic and inhibitor with Lipofectamine 2000 (Thermo Fisher Scientific, Waltham MA). Transfection was carried out in the same direction as the miRNA alteration in the PPHN PAECs. Since miR34c was found to be upregulated, its expression was increased in control PAECs using miRNA mimic (gain-of-function) and inhibited in the PPHN PAECs using miRNA inhibitor (loss-of-function). MiR-34c mimic and inhibitor (miR-34c-5p mirVana miRNA mimic, Catalog # MC11039 and miR-34c-5p mirVana miRNA inhibitor, Catalog # MH11039, Thermo Fisher) with Lipofectamine 2000 (Thermo Fisher) was used for transfection of cultured PAECs to study effects of increasing and decreasing miR-34c expression respectively, in vitro. For experimental control, PAECs were transfected with the same concentration using the same protocol with company-provided control miRNA mimic (Thermo Fisher Catalog #4464058) and inhibitor (Thermo Fisher Catalog #4464076) that have been shown to have no physiologic effect in vitro. Real-time polymerase chain reaction (RT-PCR) was performed for miR-34c to verify differences in miR34c expression between control and PPHN PAEC and the efficacy of transfection with mimic and inhibitor (Supplementary Figs. 1–3). Cells were either harvested for RNA and protein extraction or used for cell count, migration studies, and tube formation assays after 48 h of transfection as described below.

Polymerase chain reaction (PCR) for microRNA and mRNA

Total RNA was extracted using chloroform extraction method from cells suspended in TRIzol as described previously.[5,24] This was used to prepare cDNA using Qiagen miScript II RT-PCR kit for amplification of miRNA sequences and a SuperScript kit for mRNA (Thermo Fisher) sequences using company-provided protocols. RT-PCR was performed using SYBR Green method. ΔΔCt method was used for the analysis of transcript abundance. RT-PCR was done on RNA from control and PPHN samples for comparison of miR34c levels and to verify the transfection with miR34c mimic and inhibitor (Supplementary Figs. 1–3).

Immunoblotting

Comparison of control and PPHN PAEC for Notch1 expression was done in three control (one male and two female) and 3 PPHN (two male and one female) samples. Each sample lysate was run in duplicate on the same gel; sample size of three each was used for comparison of control and PPHN groups for Notch1/β-actin ratio. Transfection of control PAEC with miR34c mimic and PPHN PAEC with miR34c inhibitor was done in PAEC from lambs

with the same-sex distribution. For comparison of control and PPHN PAEC for Hey1 and Hes1 expression, lysates from four control and four PPHN PAEC (two each of male and female sex) were used. After aspirating media from culture dishes, adherent cells were washed with Hank's Balanced Salt Solution (HBSS) and scraped using a cell scraper. Cell lysates were prepared in radioimmunoprecipitation assay buffer and heat stabilized after adding Laemmli buffer at 95 °C for 10 min. Twenty microgram of protein lysate was resolved by sodium dodecyl sulfate-polyacrylamide gels for electrophoresis. Gels were run at 100 V, transferred onto nitrocellulose membranes, and blocked using 3% bovine serum albumin blocking buffer. Membranes were probed with primary antibodies overnight at 4 °C, washed with Tris-buffered Saline with 0.1% Tween-20 (TBST) buffer, incubated with horseradish peroxidase (HRP)-conjugated secondary antibodies (1:5000 of goat anti-rabbit or anti-mouse) to the primary antibody for 1 h at room temperature and washed with TBST again. For signal generation, HRP enzyme activity was detected using Pierce ECL Western Blotting Substrate (Thermo Fisher Scientific Inc.) and recorded on iBright FL1000 Imaging System (Thermo Fisher Scientific Inc). Images were analyzed using ImageJ and normalized to beta-actin. Primary antibodies used were rabbit Notch1 (1:1000, Abcam #ab52627), rabbit Hey1 (1:1000, Abcam catalog # 154077), and rabbit Hes1 (1:1000, Abcam catalog # ab71559).

Angiogenesis assays

Since the primary cellular processes affected by miR34c, which is the focus of our study include angiogenesis functions of cell proliferation, migration, and differentiation, we studied these functions of PAEC in vitro. For cell count and viability, adherent cells were detached from culture dishes using TrypLE (Thermo Fisher), centrifuged, and resuspended in DMEM. Ten microliter of resuspended cells were stained with 0.4% Trypan blue and counted for the number of live cells as well as viability using EVE Automated Cell Counter (NanoEntek, Seoul, South Korea) in triplicate for each sample.

Cell migration assay. Media was aspirated from the confluent culture dish, and a linear scratch was made in the center of the cell monolayer using a sterile 1000 µL pipette tip. The Detached cells were washed away with sterile HBSS and adherent cells were incubated in reduced serum media for 5–6 h. The width of the scratch was measured at a specific location along the line of scratch, both at the time of making the scratch and after 5–6 h of migration of cells into the gap, as reported previously.[2–4]

Capillary tube formation assay. Cells were harvested at the end of the transfection period using TrypLE to detach them from adherent monolayer and re-seeded onto 6-well plates coated with Matrigel (Corning Life Sciences, Arizona, US) at a density of 1×10^5/well in reduced serum media. After 4–6 h, media was aspirated, cells were stained with CalceinAM dye (Thermo Fisher) and visualized under fluorescent microscopy as we reported previously.[4] CalceinAM is non-fluorescent at baseline and after uptake into live cells, undergoes intracellular ester hydrolysis to form Calcein, which is a fluorochrome. Calcein is hydrophilic alcohol and hence emits green fluorescence in live cells, facilitating the identification of tube formation activity. Three images each from three separate parts of each well were obtained and analyzed using ImageJ analyzer for number of nodes, number of meshes, and total branching length.

Statistical analysis. All data are shown as mean ± SD. GraphPad Prism version 9.0 (GraphPad Software, San Diego, CA) was used for the statistical analysis of data. Unpaired *t*-test was used to compare two samples (control versus PPHN) while ANOVA was used to compare data from more than two samples (control and PPHN samples with miR mimic and anti-miR) with Tukey's post-hoc test to determine which means were different.

RESULTS

MiRNAs are differentially expressed between control and PPHN PAECs

Small RNA sequencing identified 470 differentially expressed miRNAs (DE-miRNAs) between control and PPHN PAECs (Table 1). Twelve of these were significantly different out of which seven were upregulated and five were downregulated. IPA showed that top molecular and cellular functions affected by the DE-miRNAs were cellular development, cell growth and proliferation, cellular movement, cell cycle, and cell death and survival. These are key processes involved in sprouting angiogenesis and have been implicated in the pathogenesis of pulmonary hypertension. Pathway analysis also identified the top five diseases and biological functions involved to be organismal injury, cancer, respiratory disease, cellular development, and cell movement (Fig. 1). Pathway analysis showed that the top analysis-ready miRNA was miR-34c-5p among upregulated and miR-331–5p among downregulated. This led us to select miR-34c for further studies in PPHN angiogenesis.

MiR-34c alters angiogenesis in endothelial cells in vitro

MiR-34c-5p (miR-34c) was upregulated by $\log_2$1.85 fold in PPHN PAECs as compared to control PAECs (Table 1 and Supplementary Fig. 1). IPA, TargetScan, and mirdb.org predicted 7mer-m8 canonical binding of miR-34c to the 3′UTRs of Notch1, the receptor that binds five Notch ligands and coordinates the response. Notch1 has been implicated in dysregulated angiogenesis seen in tumorigenesis as well as in pulmonary hypertension. As a result, we focused our studies on the role of miR-34c and its effects on Notch1 in PPHN.

Control lamb PAECs transfected with miR34c mimic (Supplementary Fig. 2) showed significantly decreased cell proliferation, cell migration, and tube formation in Matrigel assay as compared to those transected with control miRNA (Fig. 2 and Table 2). In contrast, PPHN PAECs, which have decreased angiogenesis at baseline showed improved cell proliferation, cell migration, and tube formation when transfected with miR-34c inhibitor (Supplementary Fig. 3) as compared to control miRNA inhibitor (Fig. 2 and Table 2).

PPHN PAECs show decreased expression of Notch1 and its downstream targets

To identify whether Notch1 is a potential target of miR-34c, we aimed to first identify the role of Notch1 in PPHN. We found that Notch1 protein expression was significantly decreased in PPHN PAECs as compared to control PAECs (Fig. 3a, c). We also investigated the downstream transcriptional targets of Notch1 intracellular domain (N1 ICD), Hey1, and Hes1. We found that Hey1 and Hes1 were significantly decreased in PPHN PAECs as compared to control PAECs (Fig. 3b, c).

Table 1. Significantly differentially expressed miRNAs between PPHN and control PAECs with $n = 6$ of each of control and PPHN lambs.

microRNA	$\log_2$(fold change)	Neg $\log_2$Q value (false discovery rate)
miR-26b	−0.505	17.34
miR-30b	−0.464	11.62
miR-2779	−1.562	11.23
miR-331–5p	−1.002	10.42
miR-874	1.205	8.34
miR-125a-5p	0.743	8.33
miR-2387	1.538	7.32
miR-1692	1.906	5.31
miR-34c-5p	1.855	5.31
miR-361-5p	0.603	5.31
miR-2340	2.925	5.10
miR-342	−0.494	5.10

Negative $\log_2$Q value = 4.32 was determined as significant (which corresponds to Q value of 0.05). MiRNAs are arranged according to decreasing order of level of significance. MiRNAs with a negative value of $\log_2$(fold change) were downregulated and those with a positive value were upregulated.

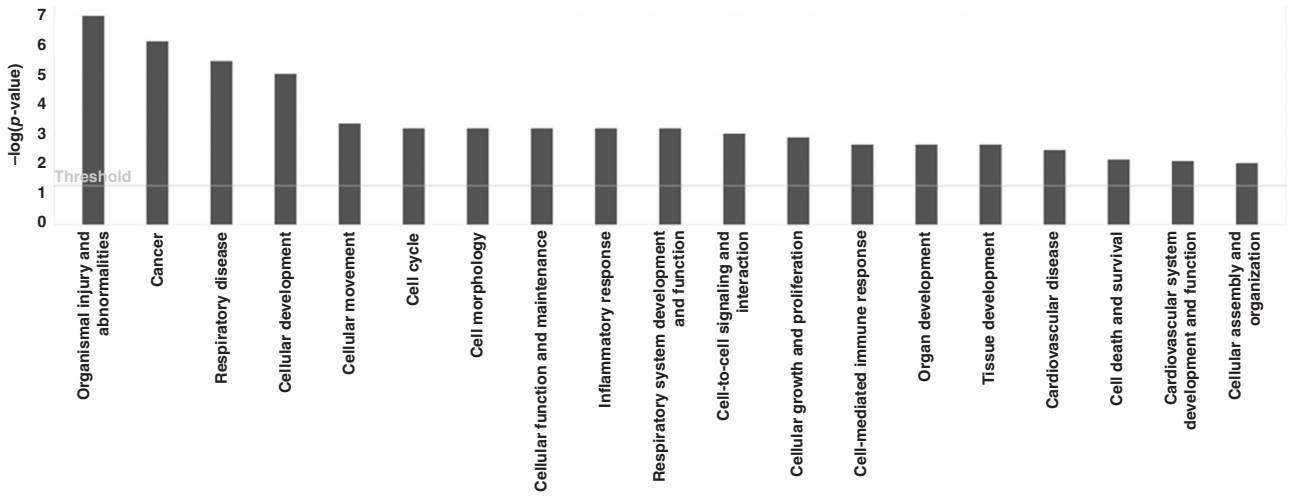

Fig. 1 Physiologic pathways affected by miRNA differentially expressed in PPHN. Key mechanisms and functions that are affected by the differentially expressed miRNAs between control and PPHN PAECs based on ingenuity pathway analysis.

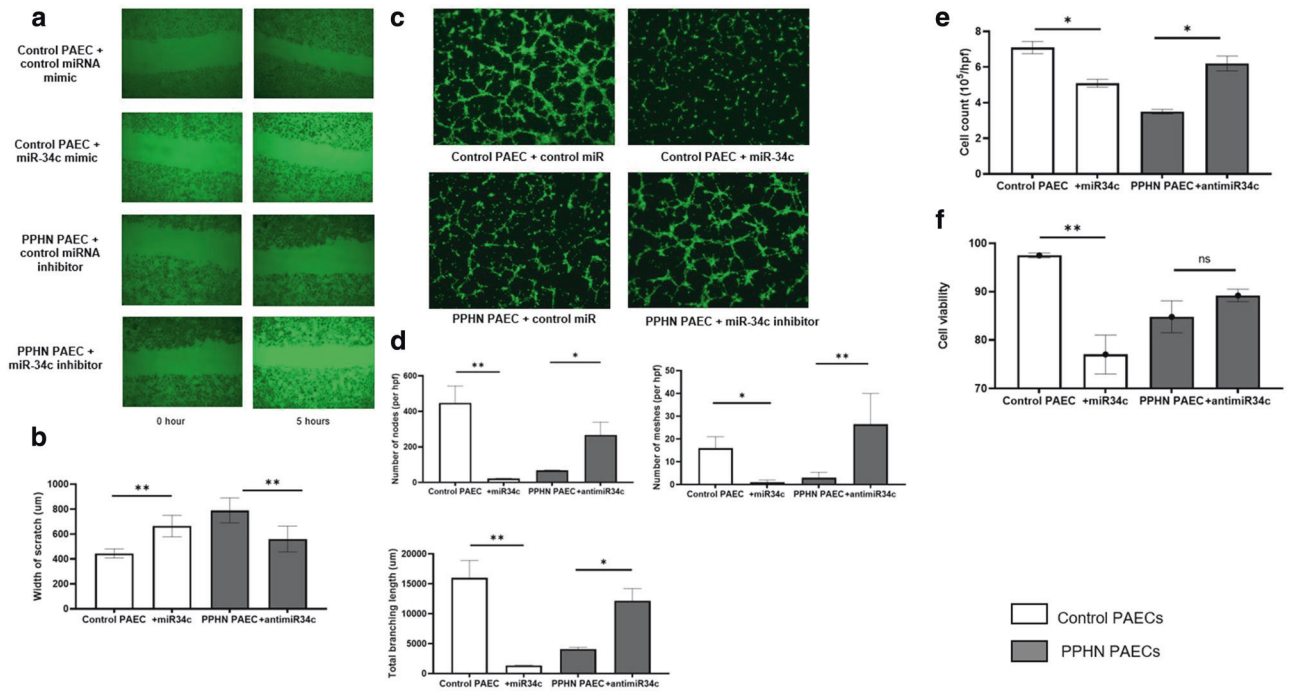

Fig. 2 In vitro angiogenesis function of PAECs. a Cell migration assay for control and PPHN pulmonary artery endothelial cells (PAECs) under fluorescent microscopy. First column represents images taken immediately after monolayer scratch and second column are images taken 5 h after recovery with migration of cells across the margins during incubation in reduced serum media. **b** Summarized data for the difference in the width of scratch in μM between different groups after normalizing to the initial width. Data are mean ± SD for $n = 3$ and ** indicates $p < 0.01$. **c** Images of capillary tube formation assay in Matrigel matrix. Control PAECs were transfected with control miRNA mimic or miR-34c mimic and PPHN PAECs were transfected with control miRNA inhibitor or miR-34c inhibitor. Both control and PPHN PAECs were obtained from three separate control lambs and Matrigel assay was performed in triplicate for each and averaged. Assay was analyzed using ImageJ and final analyses was performed on number of nodes, meshes, and total branching length as shown in panel **d** by ANOVA and Tukey's post-hoc test. *$p < 0.05$ and **$p < 0.01$. **e** Analysis of cell count after 48 h of transfection of control and PPHN PAECs with miR34c mimic and anti-miR34c, respectively. Analysis was done for control PAEC/control mimic vs control PAEC/miR-34c mimic and for PPHN PAEC/control inhibitor vs PPHN PAEC/miR-34c inhibitor for $n = 3$ each by ANOVA and Tukey's post-hoc test. *$p < 0.05$ for both comparisons. **f** Analysis of cell viability measured using Eve automated cell counter after staining cells with 0.4% Trypan blue post 48 h of transfection. Data are mean ± SD for $n = 3$ for each cell/transfection type and represented as shown in Table 2 and figure. White bars represent control PAECs and gray bars represent PPHN PAECs. **$p < 0.01$ by ANOVA and Tukey's post-hoc test.

MiR-34c overexpression decreases mRNA and protein expression of Notch1 and its downstream targets in control PAECs and anti-miR34C increases them in PPHN PAECs

RT-PCR for Notch1 mRNA (forward primer CAAGAAGTTCCGGTTC-GAGGA, reverse primer TGTCTGGTCGTCCAGGTCAG) in control PAECs transfected with miR-34c mimic showed significantly decreased levels of the Notch1 transcript ($n = 5$, $p = 0.0079$), thereby indicating that miR-34c overexpression likely leads to degradation of Notch1 transcript.

Notch1 protein expression was significantly decreased with the addition of miR-34c mimic in control PAECs (Fig. 3a, b,

Table 2. Cell count and cell viability after 48 h of transfection of control and PPHN PAECs as shown in the table.

	Control PAEC + control mimic Mean (SD)	Control PAEC + miR-34c mimic Mean (SD)	*p* value
Cell count (10^5)	7.1 (0.34)	5.1 (0.22)	*
Percentage of live cells	97.5 (0.5)	77 (4)	**
	PPHN PAEC + control inhibitor	PPHN PAEC + miR-34c inhibitor	
Cell count (10^5)	3.5 (0.13)	6.2 (0.42)	*
Percentage of live cells	84.8 (3.3)	89.2 (1.3)	ns

All transfections were carried out with PAECs obtained from three separate control and PPHN lambs each and cell count and viability were assessed in triplicate for each sample and then averaged. Cell viability was measured using Eve automated cell counter after staining cells with 0.4% Trypan blue post 48 h of transfection. Analysis was done for control PAEC/control mimic vs control PAEC/miR-34c mimic and for PPHN PAEC/control inhibitor vs PPHN PAEC/miR-34c inhibitor using *t*-test.
* denotes *p* value <0.05, ** denotes *p* value <0.01, and ns denotes not significant.

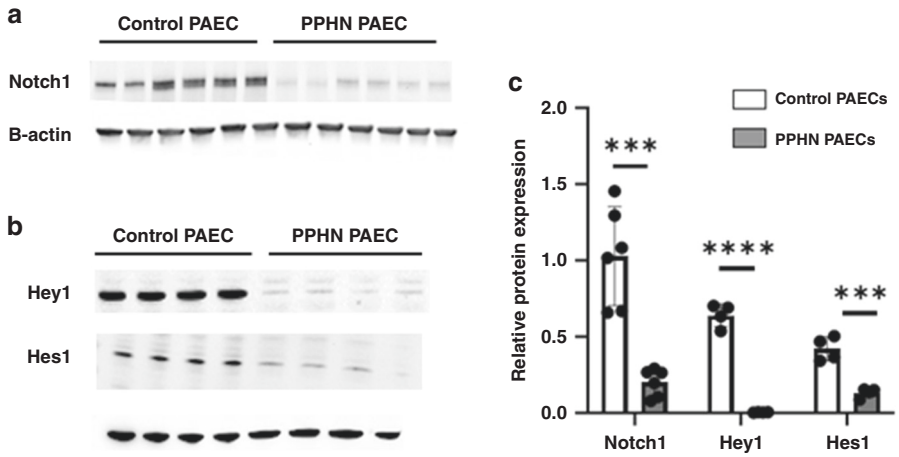

Fig. 3 Notch pathway protein expression in control and PPHN PAECs. a Immunoblotting of control and PPHN PAECs ($n = 3$ lambs for each, in duplicate in consecutive lanes) for Notch1 protein normalized to beta-actin. **b** immunoblotting for Hey1 and Hes1 protein normalized to beta-actin in control and PPHN lamb PAECs for $n = 4$ lambs each. Images were analyzed with ImageJ software. Summarized data (**c**) for Notch1 were $n = 3$ each for control and PPHN PAECs and $n = 4$ for Hey1 and Hes1 for control and PPHN PAEC shown as mean ± SD. White bars represent control PAECs and gray bars represent PPHN PAECs. Data were analyzed by unpaired *t*-test to compare expression levels for each protein in the control and PPHN PAEC. ***$p < 0.001$ for Notch1 and Hes1 and ****$p = 0.004$ for Hey1, as shown in **c**.

$n = 3$, $p < 0.05$), and the decrease in Notch1 protein expression seen in PPHN PAECs was significantly reversed by the addition of miR-34c inhibitor (Fig. 4a, b, $p < 0.01$, $n = 3$). The decrease in Notch1 expression was also found to be dose-dependent with incremental doses of the miR-34c mimic, leading to sequential decreases in the Notch1 protein expression (see Fig. 4e).

MiR-34c overexpression in control PAECs did not change the expression of Notch1 downstream targets, Hey1 and Hes1, although a trend for lower expression was noted (Fig. 4a–d, $n = 3$). In contrast, inhibition of miR-34c expression in PPHN PAECs led to increased Hey1 and not Hes1 (Fig. 4a–c, $n = 3$, $p < 0.05$ only for Hey1) expression, both of which were decreased in PPHN PAECs at baseline (Fig. 3).

DISCUSSION

Primary cellular processes predicted to involve miR-34c are apoptosis, growth, migration, proliferation, senescence, G1 phase and cell cycle progression, resistance, and differentiation based on IPA prediction tools. Accordingly, our results indicate that miR-34c regulates angiogenesis at a cellular level, likely through modulation of the canonical Notch pathway. The Notch family consists of four transmembrane Notch receptors (Notch1–4) and five ligands —Delta-like ligands–1, 3, and 4 (Dll–1, 3, 4) and Jagged (Jag) –1 and 2. Notch ligands expressed on the surface of a cell can bind to the Notch receptor of an adjacent cell, leading to its proteolytic cleavage by ADAM and gamma-secretase complex. This releases the Notch intracellular domain that is translocated to the nucleus (Fig. 5) where it interacts with the DNA-binding protein CBF1-Suppressor of Hairless-LAG1 and the co-activator Mastermind to promote gene transcription of targets belonging to the Hey and Hes family of basic helix-loop-helix proteins.[30] Notch1 is crucial for development as is evidenced by embryonic lethality in endothelial-Notch1 knockout mice with intact vasculogenesis but abnormal angiogenesis and secondary vascular remodeling.[31] Alterations in Notch receptor expression have been previously reported in the adult models of PAH.[32] A few prior studies have found an inverse relationship between miR-34c and the Notch1 expression in physiologic processes like muscle and bone development and in tumor progression.[32–34]

Notch1 has been shown to be critical in vascular development during the embryonic phase of life as evidenced by the death of endothelial-Notch1 knockout mouse embryos at E10.5.[31] Notch1 is also critical for postnatal angiogenesis and VEGF-regulated Dll4-Notch signaling establishes the adequate ratio between tip and stalk cells required for correct sprouting and branching patterns.[35,36] We previously reported that an altered balance of the Notch ligands, Jag1 and Dll4 leads to dysregulated angiogenesis in PPHN, but to our knowledge there are no reports of endothelial-Notch1 implicated in PPHN.[4] In the present study, we

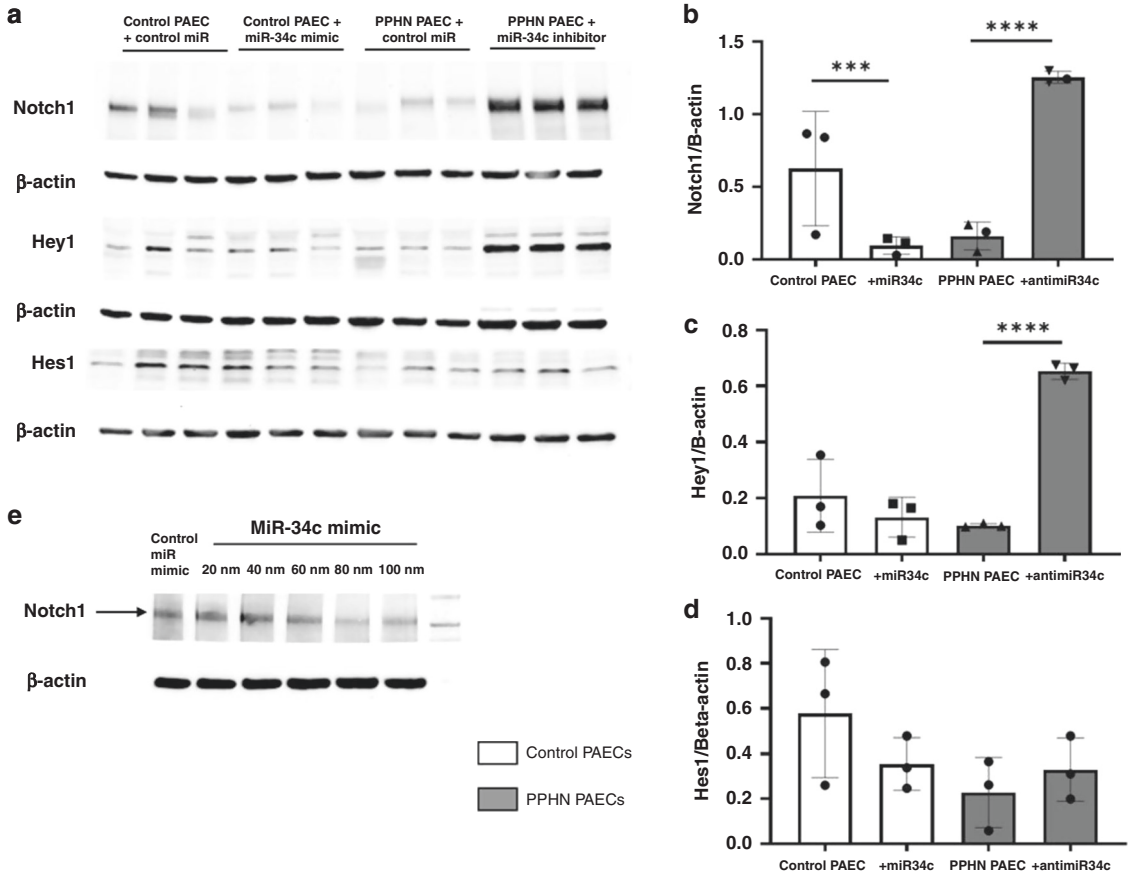

Fig. 4 Effects of miR-34c mimic and miR-34c inhibitor on Notch pathway protein expression in PAECs. a Immunoblotting for Notch1, Hey1, and Hes1 proteins in control and PPHN pulmonary artery endothelial cells transfected with miR34c mimic and inhibitors (anti-miR34c). Control PAECs and PPHN PAECs were obtained from three separate lambs each and were transfected at the same passage. Each lane represents a separate animal from which PAECs were obtained. **b**–**d** Summarized data from western blot images analyzed using ImageJ software are shown as bar graphs with mean ± SD for $n = 3$. White bars represent control PAECs and gray bars represent PPHN PAECs. Data analyzed by ANOVA and Tukey's post-hoc test. ***$p < 0.001$ and ****$p < 0.0001$. **e** Immunoblotting for Notch1 protein in control (no PPHN) PAEC lysates transfected with either control mimic (lane 1) or incremental concentrations of miR-34c mimic from 20 to 100 nM and normalized to beta-actin. Figure shows incremental decrease in Notch1 expression with increase in concentration of miR-34c used for transfection.

found that Notch1 decreased significantly in PPHN PAECs, along with the downstream targets, Hey1 and Hes1. Decrease in Notch1 is also demonstrated by increasing miR-34c expression on control PAECs and was reversed partially by inhibiting the action of miR-34c in PPHN PAECs in vitro. MiR-34c overexpression also impairs angiogenesis in control PAECs and miR-34c inhibition improves angiogenesis in PPHN PAECs. These reciprocal effects of miR34c indicate that the dysregulated angiogenesis seen in PPHN PAECs can be in part due to miR-34c overexpression in PPHN and that the effects may be mediated through Notch1 inhibition.

Hey1 and Hes1, which are downstream targets of Notch1, have been implicated in dysregulated angiogenesis. Hey1/Hey2 knock-out mice fail to express arterial endothelial markers and are essential for embryonic vascular development.[37] Endothelial-specific Hes1 mutant embryos exhibit defective vascular remodeling in the brain.[38] Our PPHN phenotype showed decreased expression of Hey1/Hes1 in the PAECs, which is likely the mechanism through which Notch1 regulates angiogenesis in this model. MiR-34c overexpression that leads to decreased Notch1 expression, also showed a decreasing trend in Hey1/Hes1 expression indicating that miR-34c-mediated Notch1 decrease affects downstream Notch signaling. Inhibition of miR-34c expression also led to increased expression of both Hey1 and Hes1 thereby indicating that loss-of-function of miR-34c leads to stimulation of Notch downstream targets as well. This effect was more pronounced in Hey1 as compared to Hes1.

Our data contrast with a recent report of increased Notch1 signaling and EC proliferation in adult PAH cells that shows downregulation of Notch2 and corresponding increase in Notch1 expression in these cells.[32] Increase in Notch1 was associated with increased Hey1 and Hes1 levels in adult PAH cells and siRNA mediated knockdown of Notch2 recapitulated the effects in control PAEC. The investigators also reported an increase in cell migration in response to decreased Notch2/increased Notch1 expression. In contrast to these findings in adult PAH, ECs in PPHN model show a consistent decrease in proliferation, migration, and tube formation and decreased angiogenesis in vitro and in vivo. We also found a decrease in Notch1 expression in PPHN and in response to miR-34c overexpression in control PAEC from fetal lambs. Other recently published studies have demonstrated the anti-proliferative effects of miR-34c in cancer cells and smooth muscle cells, similar to our findings in PAECs.[39,40] These studies highlight the importance of conducting these studies specifically in PPHN.

There are some limitations to our study. First, our studies focused on changes in miRNA expression in PAECs since we addressed changes in endothelial angiogenesis in this model. Whether miR-34c influences the proliferation and other functions of PASMCs is not clear from our studies. Since miRNAs are biologically stable in extracellular location, it is likely that they will influence other cells in pulmonary arteries. Secondly, we did not investigate the effects of miR-34c deletion or overexpression on

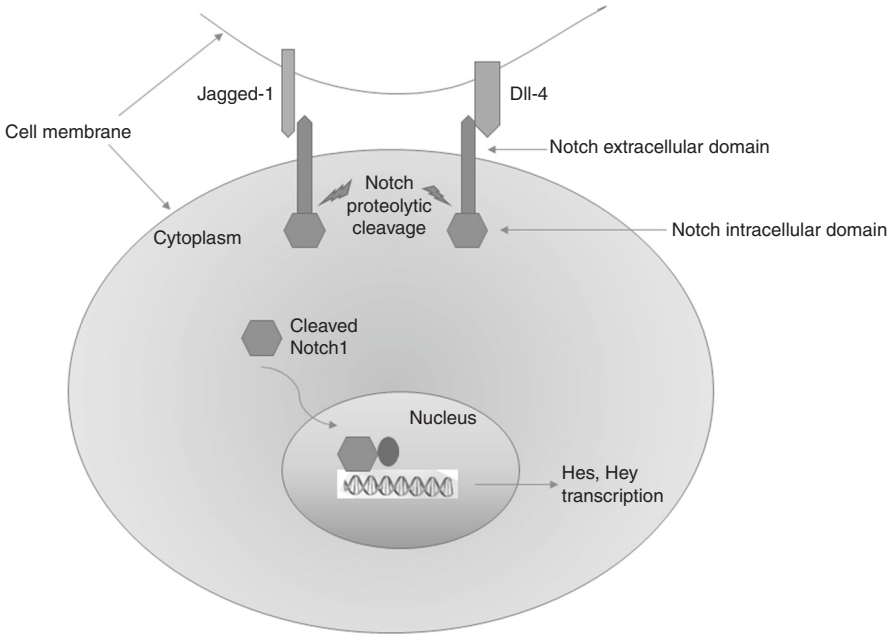

Fig. 5 Mechanism of Notch pathway signaling. Membrane-bound ligands belonging to the Jagged and Delta-like family bind the heterodimeric transmembrane Notch receptor leading to proteolytic cleavage of Notch. This leads to release of the Notch intracellular domain, which translocates to the nucleus and stimulates transcription of downstream targets belonging to Hey and Hes family of basic helix-loop-helix proteins.

angiogenesis in vivo. The larger size of the fetal lamb model and lack of genetic models precludes in vivo studies of miR-34c knockdown or overexpression in this model. We also did not study whether reversal of Notch1 downregulation in PPHN PAECs by itself, without the addition of miR-34c inhibitor improves angiogenesis. We, however, examined the role of miR34C elevation at several levels including sequencing data, angiogenesis assays, RT-PCR, and immunoblotting studies to demonstrate that miR-34c is upregulated and contributes to dysregulated angiogenesis in PPHN PAECs through the canonical Notch pathway.

In summary, we conclude that increased miR34c-5p levels in PPHN PAEC contribute to impaired angiogenesis in this model. Whether miR34C-5p-based therapies improve angiogenesis and restore postnatal adaptation in PPHN requires further studies.

DATA AVAILABILITY

The original sequencing output will be available for free download from the NCBI Sequence Read Archive after manuscript online publishing date under "Ovine PPHN PAEC smallRNA-seq" file name.

REFERENCES

1. Gien, J. et al. Chronic intrauterine pulmonary hypertension increases endothelial cell rho kinase activity and impairs angiogenesis in vitro. *Am. J. Physiol. Lung Cell Mol. Physiol.* **295**, L680–L687 (2008).
2. Teng, R. J., Eis, A., Bakhutashvili, I., Arul, N. & Konduri, G. G. Increased superoxide production contributes to the impaired angiogenesis of fetal pulmonary arteries with in utero pulmonary hypertension. *Am. J. Physiol. Lung Cell Mol. Physiol.* **297**, L184–L195 (2009).
3. Mahajan, C. N., Afolayan, A. J., Eis, A., Teng, R. J. & Konduri, G. G. Altered prostanoid metabolism contributes to impaired angiogenesis in persistent pulmonary hypertension in a fetal lamb model. *Pediatr. Res.* **77**, 455–462 (2015).
4. Rana, U. et al. Amp-kinase dysfunction alters Notch ligands to impair angiogenesis in neonatal pulmonary hypertension. *Am. J. Respir. Cell Mol. Biol.* **62**, 719–731 (2020).
5. Risau, W. Mechanisms of angiogenesis. *Nature* **386**, 671–674 (1997).
6. Gien, J., Seedorf, G. J., Balasubramaniam, V., Markham, N. & Abman, S. H. Intrauterine pulmonary hypertension impairs angiogenesis in vitro: role of vascular endothelial growth factor nitric oxide signaling. *Am. J. Respir. Crit. Care Med.* **176**, 1146–1153 (2007).
7. Teng, R. J. et al. Amp kinase activation improves angiogenesis in pulmonary artery endothelial cells with in utero pulmonary hypertension. *Am. J. Physiol. Lung Cell Mol. Physiol.* **304**, L29–L42 (2013).
8. Macfarlane, L. A. & Murphy, P. R. MicroRAN: biogenesis, function and role in cancer. *Curr. Genomics* **11**, 537–561 (2010).
9. Tetreault, N. & De Guire, V. miRNAs: their discovery, biogenesis and mechanism of action. *Clin. Biochem.* **46**, 842–845 (2013).
10. Poliseno, L. et al. MicroRNAs modulate the angiogenic properties of HUVECs. *Blood* **108**, 3068–3071 (2006).
11. Caporali, A. & Emanueli, C. MicroRNA regulation in angiogenesis. *Vasc. Pharm.* **55**, 79–86 (2011).
12. Pullamsetti, S. S. et al. Inhibition of microRNA-17 improves lung and heart function in experimental pulmonary hypertension. *Am. J. Respir. Crit. Care Med.* **185**, 409–419 (2012).
13. Boucherat, O., Potus, F. & Bonnet, S. MicroRNA and pulmonary hypertension. *Adv. Exp. Med. Biol.* **888**, 237–252 (2015).
14. Doebele, C. et al. Members of the microRNA-17-92 cluster exhibit a cell-intrinsic antiangiogenic function in endothelial cells. *Blood* **115**, 4944–4950 (2010).
15. Bonauer, A. et al. MicroRNA-92a controls angiogenesis and functional recovery of ischemic tissues in mice. *Science* **324**, 1710–1713 (2009).
16. Xu, Y. P. et al. miR-126a-5p is involved in the hypoxia-induced endothelial-to-mesenchymal transition of neonatal pulmonary hypertension. *Hypertens. Res.* **40**, 552–561 (2017).
17. Nicoli, S. et al. MicroRNA-mediated integration of haemodynamics and VEGF signalling during angiogenesis. *Nature* **464**, 1196–1200 (2010).
18. Qin, W. et al. BMPRII is a direct target of miR-21. *Acta Biochim. Biophys. Sin. (Shanghai)* **41**, 618–623 (2009).
19. Sood, B. et al. *Microrna Biomarkers in Persistent Pulmonary Hypertension of the Newborn*. https://pvrinstitute.org/media/2534/074-beena-sood.pdf (2017).
20. Konduri, G. G. & Mital, S. Adenosine and ATP cause nitric oxide-dependent pulmonary vasodilation in fetal lambs. *Biol. Neonate* **78**, 220–229 (2000).
21. Konduri, G. G. & Mattei, J. Role of oxidative phosphorylation and ATP release in mediating birth-related pulmonary vasodilation in fetal lambs. *Am. J. Physiol. Heart Circ. Physiol.* **283**, H1600–H1608 (2002).
22. Hoyer, L. W., De los Santos, R. P. & Hoyer, J. R. Antihemophilic factor antigen. Localization in endothelial cells by immunofluorescent microscopy. *J. Clin. Invest.* **52**, 2737–2744 (1973).
23. Voyta, J. C., Via, D. P., Butterfield, C. E. & Zetter, B. R. Identification and isolation of endothelial cells based on their increased uptake of acetylated-low density lipoprotein. *J. Cell Biol.* **99**, 2034–2040 (1984).
24. Rio, D. C., Ares, M. Jr., Hannon, G. J. & Nilsen, T. W. Purification of RNA using TRIzol (TRI reagent). *Cold Spring Harb. Protoc.* **2010**, pdb.prot5439 (2010).

25. Gao, F. et al. Changes in miRNA in the lung and whole blood after whole thorax irradiation in rats. *Sci. Rep.* **7**, 44132 (2017).
26. Kriegel, A. J. et al. Characteristics of microRNAs enriched in specific cell types and primary tissue types in solid organs. *Physiol. Genomics* **45**, 1144–1156 (2013).
27. Hackenberg, M., Sturm, M., Langenberger, D., Falcon-Perez, J. M. & Aransay, A. M. Miranalyzer: a microRNA detection and analysis tool for next-generation sequencing experiments. *Nucleic Acids Res.* **37**, W68–W76 (2009).
28. Agarwal, V., Bell, G. W., Nam, J. W. & Bartel, D. P. Predicting effective microRAN target sites in mammalian mRNAs. *Elife* **4**, e05005 (2015).
29. Benjamini, Y. & Hochberg, Y. Controlling the false discovery rate: a practical and powerful approach to multiple testing. *J. R. Stat. Soc. Ser. B (Methodol.)* **57**, 289–300 (1995).
30. Bray, S. J. Notch signalling in context. *Nat. Rev. Mol. Cell Biol.* **17**, 722–735 (2016).
31. Limbourg, F. P. et al. Essential role of endothelial Notch1 in angiogenesis. *Circulation* **111**, 1826–1832 (2005).
32. Bae, Y. et al. miRNA-34c regulates Notch signaling during bone development. *Hum. Mol. Genet* **21**, 2991–3000 (2012).
33. Luo, Y., Wang, D., Chen, S. & Yang, Q. The role of miR-34c-5p/Notch in epithelial-mesenchymal transition (EMT) in endometriosis. *Cell Signal* **72**, 109666 (2020).
34. Hou, L. et al. miR-34c represses muscle development by forming a regulatory loop with Notch1. *Sci. Rep.* **7**, 9346 (2017).
35. Hellstrom, M. et al. Dll4 signalling through Notch1 regulates formation of tip cells during angiogenesis. *Nature* **445**, 776–780 (2007).
36. Takeshita, K. et al. Critical role of endothelial Notch1 signaling in postnatal angiogenesis. *Circ. Res.* **100**, 70–78 (2007).
37. Fischer, A., Schumacher, N., Maier, M., Sendtner, M. & Gessler, M. The Notch target genes Hey1 and Hey2 are required for embryonic vascular development. *Genes Dev.* **18**, 901–911 (2004).
38. Kitagawa, M. et al. Hes1 and Hes5 regulate vascular remodeling and arterial specification of endothelial cells in brain vascular development. *Mech. Dev.* **130**, 458–466 (2013).
39. Wei, H. et al. miR34c5p targets Notch1 and suppresses the metastasis and invasion of cervical cancer. *Mol. Med. Rep.* **23**, 120 (2021).
40. Wan, W. F. et al. miR-34c inhibits PDGF-BB-induced HAVSMCs phenotypic transformation and proliferation via PDGFR-BETA/SIRT1 pathway. *Mol. Biol. Rep.* **48**, 4137–4151 (2021).

AUTHOR CONTRIBUTIONS

Substantial contributions to conception and design, acquisition of data, or analysis and interpretation of data: D.M., U.R., A.J.K., P.L., T.M., and G.G.K. Drafting the article or revising it critically for important intellectual content: D.M. and G.G.K. Final approval of the version to be published: D.M. and G.G.K.

FUNDING

This work was supported by grants 1R01 HL136597–01 from NHLBI, Multiyear Innovation Research grant, and Muma Endowed Chair in Neonatology from Children's Research Institute of Children's Wisconsin (G.G.K.).

COMPETING INTERESTS

The authors declare no competing interests.

ADDITIONAL INFORMATION

Supplementary information The online version contains supplementary material available at https://doi.org/10.1038/s41390-022-02151-3.

Correspondence and requests for materials should be addressed to Girija Ganesh Konduri.